Journal of Inorganic Biochemistry 194 (2019) 153–159

Contents lists available at ScienceDirect

Journal of Inorganic Biochemistry

journal homepage: www.elsevier.com/locate/jinorgbio

Synthesis, characterization and antibacterial activity of Zn(II) coordination polymer

Dongming Wang, Xiaowei Xing, Xiaomei Ye, Zhi Chen, Zhanping Gou, Dudu Wu*

School of Pharmacy, Guangdong Medical University, Dongguan 523808, China

ARTICLE INFO

Keywords:
Zinc-based coordination polymer
Synthesis
Antibacterial activity

ABSTRACT

In this study, the zinc(II)-based coordination polymer, $[Zn(CPDA)(NO_3)_2)]$(CPDA = 1,2-cyclopentanedicarboxylic acid) (1), had been successfully synthesized according to the hydrothermal method. Afterwards, 1 had been characterized by means of single crystal and power X-ray diffraction, elemental analysis, thermogravimetric analysis and infrared spectrum techniques. In addition, the antibacterial activities in vitro had been evaluated towards *Escherichia coli* (*E. coli*) and *Staphylococcus aureus* (*S. aureus*), respectively, through the growth inhibition and inhibition zone experimental methods. Our results indicated that 1 had displayed favorable antibacterial activity compared with the Zinc nitrate and the CPDA ligand. These findings had revealed that the antibacterial mechanism of 1 might be correlated with the production of reactive oxygen species (ROS) in cells.

1. Introduction

Microbial infection remains one of the leading causes of deaths for the population worldwide. Notably, it is reckoned that 26% of the global death toll would be induced by infectious diseases; particularly, 50–52% people in sub-Saharan Africa have died of AIDS [1]. Obviously, it is of crucial importance to resist against the microbial activity. Typically, some coordination polymers (CPs) among the antibacterial agents have also been used for microbial resistance. CPs represent a novel type of organic-inorganic hybrid materials, which are associated with a huge potential for extensive applications, such as in catalysis, drug delivery, magnetism, fluorescence, sensing, pollutant adsorption, and anti-bacteria [2–11], thanks to their active sites, readily tailored structures as well as various compositions [12]. Notably, the metal CPs utilized to resist against microorganism have aroused great interests from people, some of which have been synthesized and investigated, including the antifungal, antiviral, antitumor and antibacterial agents [13–16]. Particularly, for antibacterial agents, Lu et al. had constructed 4 silver-based CPs from 1H-benzimidazole to resist against *E. coli* and *S. aureus*, which had displayed broad antibacterial capabilities [17]. Moreover, Dhayabaran et al. had reported 4 novel Co(II), Cu(II), Ni(II) and Zn(II) complexes with the schiff base ligand derived from histidine and 1,3-indandione, which had shown higher antibacterial activities against bacteria than against fungi [18]. Noteworthily, among these transition metal elements, zinc is one of the most extensively used biological metal ions from the perspective of anti-bacteria [19,20]. For instance, Taghizade et al. had prepared 3 novel zinc halide complexes with the new bidentate schiff base ligand to combat various bacteria as well as fungi, which had displayed high antimicrobial activities in vitro [21]. Besides, Hongyan et al. demonstrated that, the novel antibiofilm agents zinc-protoporphyrin IX or zinc-mesoprotoporphyrin IX, were remarkably effective on suppressing the growth of suspended bacteria [22]. Therefore, it would be of great significance to use the zinc-based CPs as the potent antibacterial agents. On the other hand, the carboxylic acid complexes also exhibit high antimicrobial activities. For example, Stathopoulou et al. had reported that the antimicrobial activities of $[Ag(salH)]_2$ ($salH_2$ = salicylic acid) towards *Pseudomonas aeruginosa*, *Staphylococcus epidermidis* and *Staphylococcus aureus*, were higher than those of $AgNO_3$ or $salH_2$ [23]. In addition, Aldabaldetrecu et al. had designed 5 silver carboxylate complexes to resist against *Staphylococcus epidermidis,* and they had found that these complexes showed multiple antibacterial properties [24]. Therefore, 1,2-cyclopentanedicarboxylic acid (CPDA), a model dicarboxylic acid, had been selected as the ligand in this study, so as to improve the antibacterial activity of CPs.

In this paper, zinc(II) and 1,2-cyclopentadienoic acid (CPDA) had been reacted and synthesized $[Zn(CPDA)(NO_3)_2)]$ under the solvothermal conditions. Thereafter, the structure of **1** would be characterized by means of power X-ray diffraction (PXRD), elemental analysis (EA), thermogravimetric analysis (TGA) and Fourier Transform Infrared Spectroscopy (FTIR). Additionally, **1** had been proved to have favorable antibacterial efficacy towards different microorganisms,

* Corresponding author.
E-mail address: wududuwdd@126.com (D. Wu).

https://doi.org/10.1016/j.jinorgbio.2019.02.014
Received 21 November 2018; Received in revised form 25 February 2019; Accepted 26 February 2019
Available online 27 February 2019

including *E.coli* and *S. aureus*; eventually, ROS involvement in the antibacterial mechanism of **1** had also been examined.

2. Materials and methods

2.1. Materials and reagents

Zinc nitrate hexahydrate ($Zn(NO_3)_2{\cdot}6H_2O$) had been purchased from Xilong Science Co. Ltd. 1,2-cyclopentanedicarboxylic acid (CPDA) was bought from Beijing Huawei Ruike Chemical Co. Ltd. *N*, *N*-Dimethylformamide (DMF), 2′, 7′-dichlorofluorescein diacetate (DCFH-DA) and *N*-acetylcysteine (NAC) were derived from Sigma-Aldrich. LB agar powder and Reactive Oxygen Species Assay Kit were provided by Beijing Solarbio Science & Technology Co. Ltd. Yeast extract and Tryptone had been obtained from English OxOid Corporation. Sodium chloride (NaCl) was provided by Tianjin Damao Chemical Reagent Factory. Gentamycin was obtained from Shanghai Fusheng Industrial Co. Ltd. All chemical reagents used in this study were at analytical grade, which would not be further purified. In addition, the doubly deionized water had been applied in the preparation of all solutions. Both *E. coli* (ATCC 52922) and *S. aureus* (ATCC 25923) had been provided by Guangdong Huan Kai Microbiology Technology Co. Ltd.

2.2. Synthesis of compound *1*

Briefly, 0.12 g $Zn(NO_3)_2{\cdot}6H_2O$ (0.40 mmol) and 0.06 g 1,2-cyclopentanedicarboxylic acid (0.40 mmol) were added into the mixed solvent supplemented with DMF-H_2O (1:2) in a beaker, and the mixture would then be stirred evenly for 30 min using a magnetic stirrer. Subsequently, the resultant solution would be transferred to a 20 mL Teflon-lined stainless steel reactor, which was then heated at 150 °C for 48 h under autogenous pressure. After cooling down to room temperature for 24 h and filtering out, all colorless mass crystals would be gathered, washed with absolute ethanol for about 4 times and dried in air.

2.3. Crystallographic analysis

X-ray diffraction (XRD) data of **1** were collected from the Bruker-AXS SMART CCD area detector diffractometer equipped with ω-scan and Mo-Kα radiation (λ = 0.71073) at room temperature. The structures would then be analyzed through direct methods, followed by further refinement by the full-matrix least-squares on the foundation of F^2 using the SHELXL software [25]. Moreover, the whole matrix would be optimized through the least square method. Additionally, all non-hydrogen atoms would be treated with anisotropic thermal parameters and the hydrogen atoms would be computed through the geometrical models.

TGA was performed using the Shimadzu 51/51H, in which the thermal analyzer would be heated from 0 °C to 800 °C in air at a heating rate of 10 °C/min. Moreover, the FTIR spectra would be recorded within the 4000–1000 cm^{-1} region using the Nicolet Magna 550II Fourier-transform infrared spectrometer; at the same time, 128 scans with a resolution of 4 cm^{-1} would be collected simultaneously.

2.4. Antibacterial experiment

In this study, the antibacterial activities of **1** would be tested against two bacteria through measuring their growth inhibition curves at different concentrations within the LB broth medium (LB, containing 5 $g{\cdot}mL^{-1}$ yeast extract, 10 $g{\cdot}mL^{-1}$ sodium chloride as well as 10 $g{\cdot}mL^{-1}$ tryptone). All experiments had been performed under dark conditions. In the growth curve test, a 5 mL sterile solution mixer containing LB broth medium with different concentrations of **1** had been prepared at first, followed by the inoculation of 50 μL microorganism culture at the culture concentration of about 1.0×10^7 colony forming units per milliliter (CFU/mL). Subsequently, bacteria were grown in a shaker at 37 °C. Typically, the optical density at 600 nm (OD_{600}) of all samples in the 10 mm quartz cuvette would be measured through a spectrophotometer at the preordained time intervals, so as to determine the growth curves. However, the bacterial growth curves without any additional antibacterial agents had been tested as the negative controls, and the growth curve of positive control experiments would be measured in the presence of gentamycin.

Besides, the zone of inhibition (ZOI) would be measured according to the disc diffusion method [26]. Moreover, the mixture of autoclaved LB broth medium and dissolved agar would be solidified on the sterilized Petri dishes. On the other hand, the microorganisms to be tested (approximately 1.0×10^7 CFU/mL) that were activated in liquid LB broth medium would be evenly diffused on the LB solid medium surface. Afterwards, the filter discs impregnated with 10 μL corresponding sample solutions would be placed onto the agar surface in each plate; by contrast, the filter discs of the negative control would only be infiltrated with an equivalent amount of LB liquid, with no additional sample supplement. Thereafter, these plates were subject to standing at 4 °C for 2 h before incubation at 37 °C for 24 h. In addition, the ZOI diameter was measured through subtracting the disc diameter from the total ZOI diameter [27]. All tests had been repeated for three times under the same setting conditions.

To find out the potential mechanism underlying the antibacterial activity of **1**, 2′, 7′-dichlorofluorescein diacetate (DCFH-DA) had been used as the fluorescent probe to analyze the production of reactive oxygen species (ROS) by *E. coli* and *S. aureus*. Specifically, DCFH-DA without fluorescence could freely pass through the cell membrane, which would be subsequently hydrolyzed by intracellular esterases to form 2′,7′-dichlorodihydrofluorescein (DCFH) and would not pass through the cell membrane any more. Afterwards, the non-fluorescent DCFH would be oxidized to the high fluorescent 2′,7′-dichlorofluorescein (DCF) by ROS in cells [28,29]. Consequently, the ROS production in microorganism could be estimated through detecting the DCF fluorescence amount.

3. Results and discussion

3.1. Crystal structure of *1*

As for the structure of **1**, PXRD study suggested that it had crystallized in the tetragonal system, with the space group of P4/nmm. Besides, the fundamental building unit of **1** had contained a single Zn^{2+} and a CPDA ligand. In addition, Zn^{2+} was six-coordinated by the oxygen atoms from the carboxyl groups of CPDA (Scheme 1). The crystallographically independent unit had connected each other by means of the ligand, which had formed the 1D chain whose structure

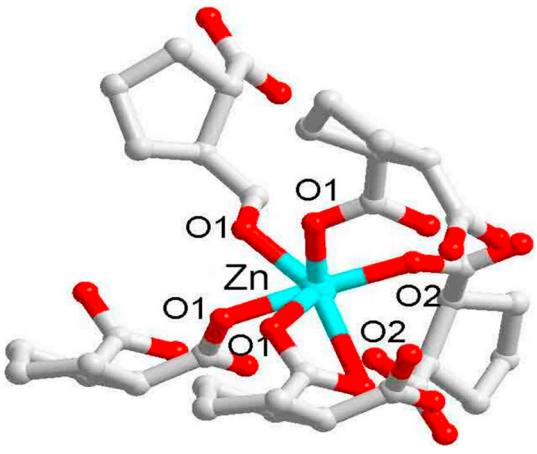

Scheme 1. Structure of complex **1**.

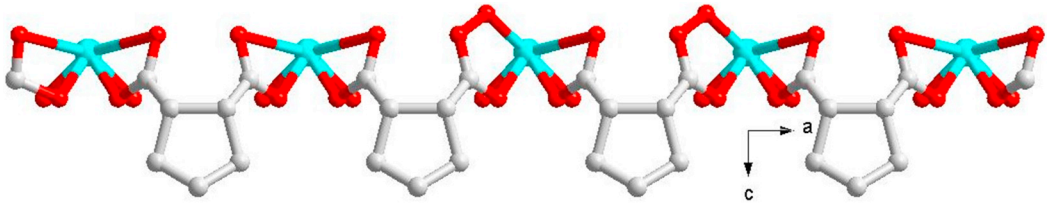

Scheme 2. One-dimensional chain structure of **1**.

Table 1
Crystallographic data and structure refinement for **1**.

Empirical formula	$C_7H_6O_4Zn$
Formula weight	219.50
Crystal system	Tetragonal
Space group	P 4/n m m
a (Å)	6.1490 (9)
b (Å)	6.1490 (9)
c (Å)	10.460 (3)
α (°)	90
β (°)	90
γ (°)	90
Unit cell volume (Å3)	395.5 (2)
Temperature (K)	100.15
Z	2
Dcalcd (g/cm3)	1.860
μ (mm–1)	3.072
F (000)	224.0
θ Range (°)	3.844–27.564
Reflection collected	2930
Independent reflections (Rint)	0.0331
Goodness-of-fit on F^2	1.150
$R1$, wR_2 ($I > 2\sigma(I)$) *	0.0260, 0.0679
$R1$, wR_2 (all data) **	0.0292, 0.0697

*$R = \Sigma(F_o - F_c)/\Sigma(F_o)$.
**$wR_2 = \{\Sigma[w\ (Fo^2–Fc^2)\ ^2]/\Sigma(Fo\ ^2)^2\}^{1/2}$.

Table 2
Selected bond distances and angles of **1**.

Bond lengths (Å)	
Zn(1)-O(1) #1	1.969(6)
Zn(1)-O(2) #2	1.949(4)
O(1)-O(1) #1	0.602(17)
O(1)-C(1)	1.257(10)
O(2)-C(5)	1.279(8)
C(1)-C(2)	1.468(9)
C(2)-C(3)	1.540(9)
C(3)-C(4)	1.465(11)
Bond angles (°)	
O(1)-Zn(1)-O(1) #3	64.97(18)
O(2)-Zn(1)-O(1) #4	119.3(2)
O(1)-O(1)-Zn(1) #1	81.2(2)
C(1)-O(1)-Zn(1)	113.3(5)
O(1)-C(1)-O(2)	120.2(7)
O(1)-C(1)-C(2)	119.7(6)
C(1)-C(2)-C(3)	115.5(5)
C(4)-C(3)-C(2)	105.2(7)

#1:y,x,z; #2:x + 1/2,y + 1/2,-z + 1; #3:y,-x + 3/2,z; #4:-y + 1,x + 1/2,-z + 1.

would be formed through connecting the Zn−O bonds (Scheme 2). Details regarding the collection of crystallographic data and refinement parameters are summarized in Table 1; meanwhile, the selected bond distances and bond angles are presented in Table 2.

3.2. PXRD, TGA and FTIR

Fig.1 has displayed the PXRD pattern of the synthesized sample **1**. As could be observed, the maximum peak positions of the experimental patterns could be obtained, which had corresponded to the simulation

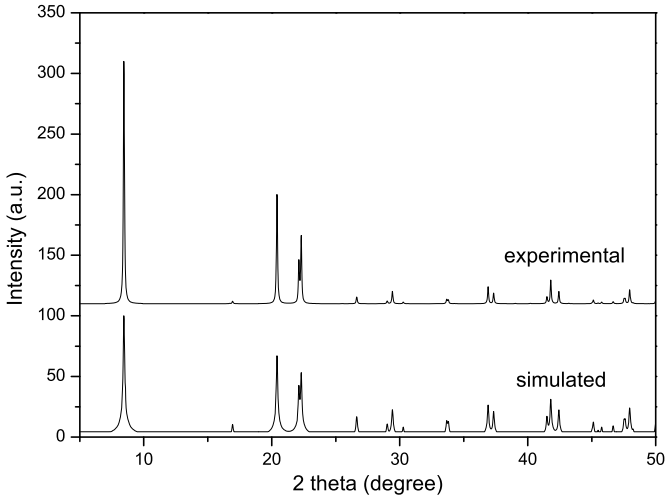

Fig. 1. PXRD pattern of **1**.

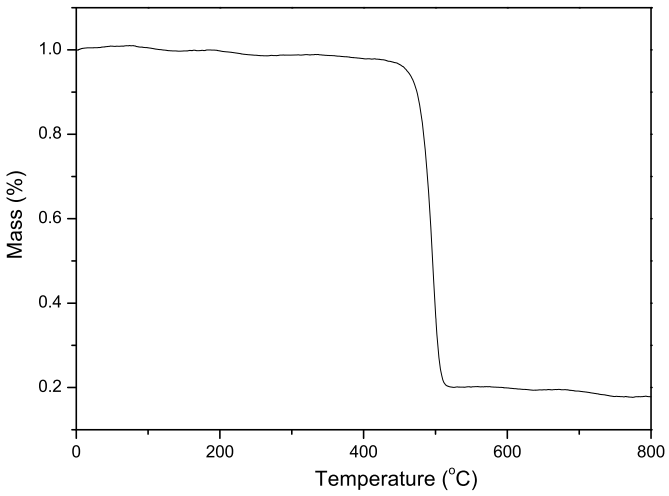

Fig. 2. TGA curve of **1**.

results from single crystal data, demonstrating that the synthesized product had a high purity.

Afterwards, the thermal stability of **1** had also been investigated by TGA under N_2 atmosphere (Fig. 2). As could be observed, **1** had undergone two stages of weight losses, among which, the first stage could be observed at the range of 100–450 °C with the weight loss of 5.1% (calc. 4.9%), and it had coincidentally corresponded to the loss of the coordinated water molecules. Meanwhile, the other stage of weight loss at 500 °C might be ascribed to the eliminated coordinated CPDA (calcd. 72.8%; found 73.8%). Finally, the residual mass was 21.1%, which nearly indicated the formation of ZnO (calcd. 22.2%).

Fig. 3 has displayed the IR spectra of CPDA and **1**. As could be observed in Fig. 3 (a), the band at 1700 cm^{-1} could be detected in the IR spectra of CPDA, which could be assigned to the stretching vibration of C=O in the carboxyl group. However, after the conjugation of CPDA

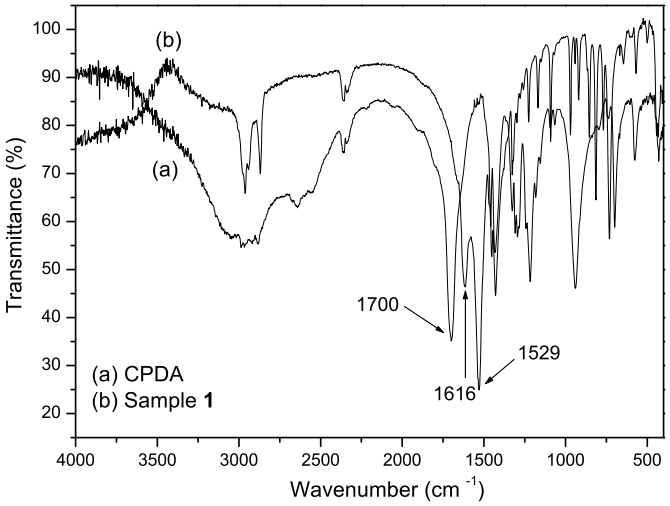

Fig. 3. FTIR spectra of CPDA and **1**.

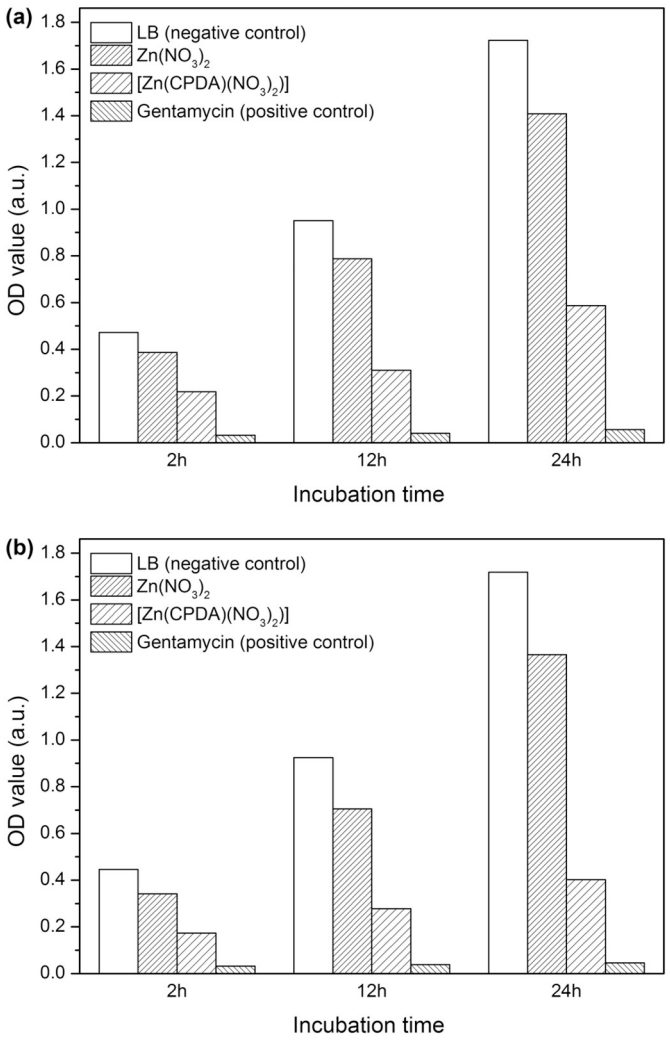

Fig. 4. The OD values of antibacterial activity for four antibacterial agents with the concentration of 20 mg·L^{-1} observed to against bacteria. (a) *E. coli*; (b) *S. aureus*.

with Zn^{2+} ions, the typical carboxyl absorption peaks had disappeared, and two new absorption peaks could be observed at 1716 cm^{-1} and 1529 cm^{-1}, respectively, in the IR spectrum of **1** (Fig.3 (b)). These new

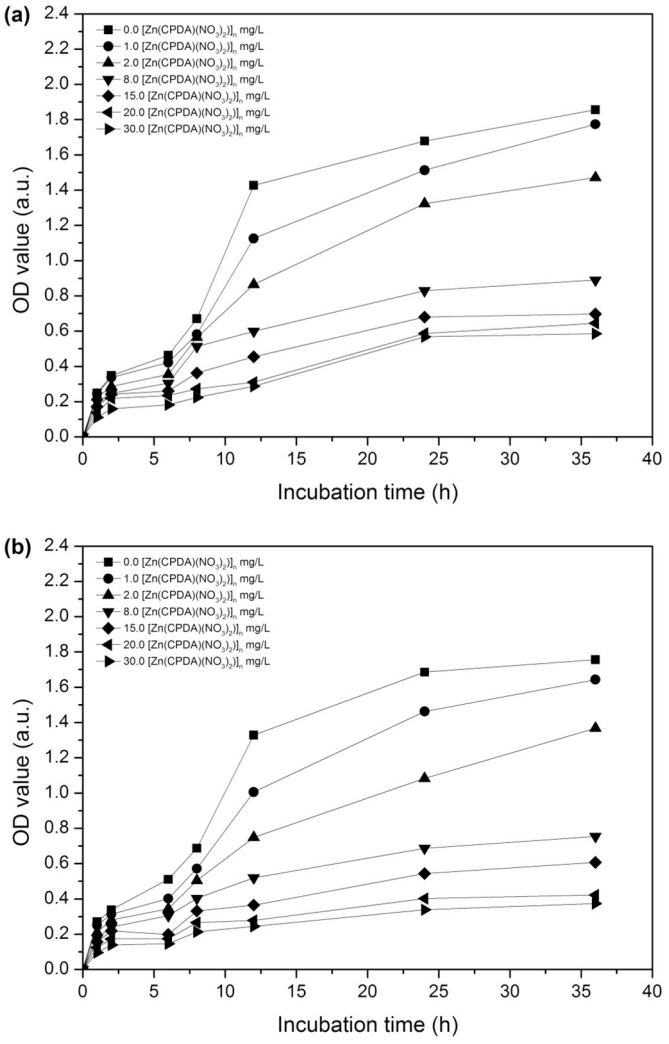

Fig. 5. Growth curves of bacteria in [Zn(CPDA)(NO$_3$)$_2$)] with different concentrations. (a) *E. coli*; (b) *S. aureus*.

peaks could be assigned to the strong C═O asymmetric stretching vibration from carboxylate, indicating that CPDA had been successfully anchored to Zn^{2+} .

3.3. Antibacterial activity of *1*

Fig. 4 has presented the antibacterial activity of Zn(NO$_3$)$_2$, **1** and gentamycin. By measuring the OD values, it was observed in this study that the OD values were increased rapidly when two bacteria had been cultured in the LB negative control, suggesting no growth suppression in the culture without **1**. Conversely, when the bacteria were cultured with gentamicin, the OD values were increased slowly, demonstrating that gentamycin was a fabulous antibacterial agent, which could serve as the standard antibiotics for antibacterial activity. Particularly, the OD values of **1** were higher than those of gentamycin but lower than those of negative control, indicating that **1** had favorable antibacterial efficacy towards different microorganisms, including *E.coli* and *S. aureus*. However, the other OD values in Zn(NO$_3$)$_2$ were relatively higher, which were closed to those of negative control, and might be due to the single influence of Zn^{2+} [30].

Fig.5 has exhibited the growth curves of two bacteria in LB broth agar plates containing **1** at various concentrations at different time points. As could be observed from the data, both concentrations and time would result in growth inhibition to a certain degree. Besides, the number of bacteria had grown quickly at low concentrations

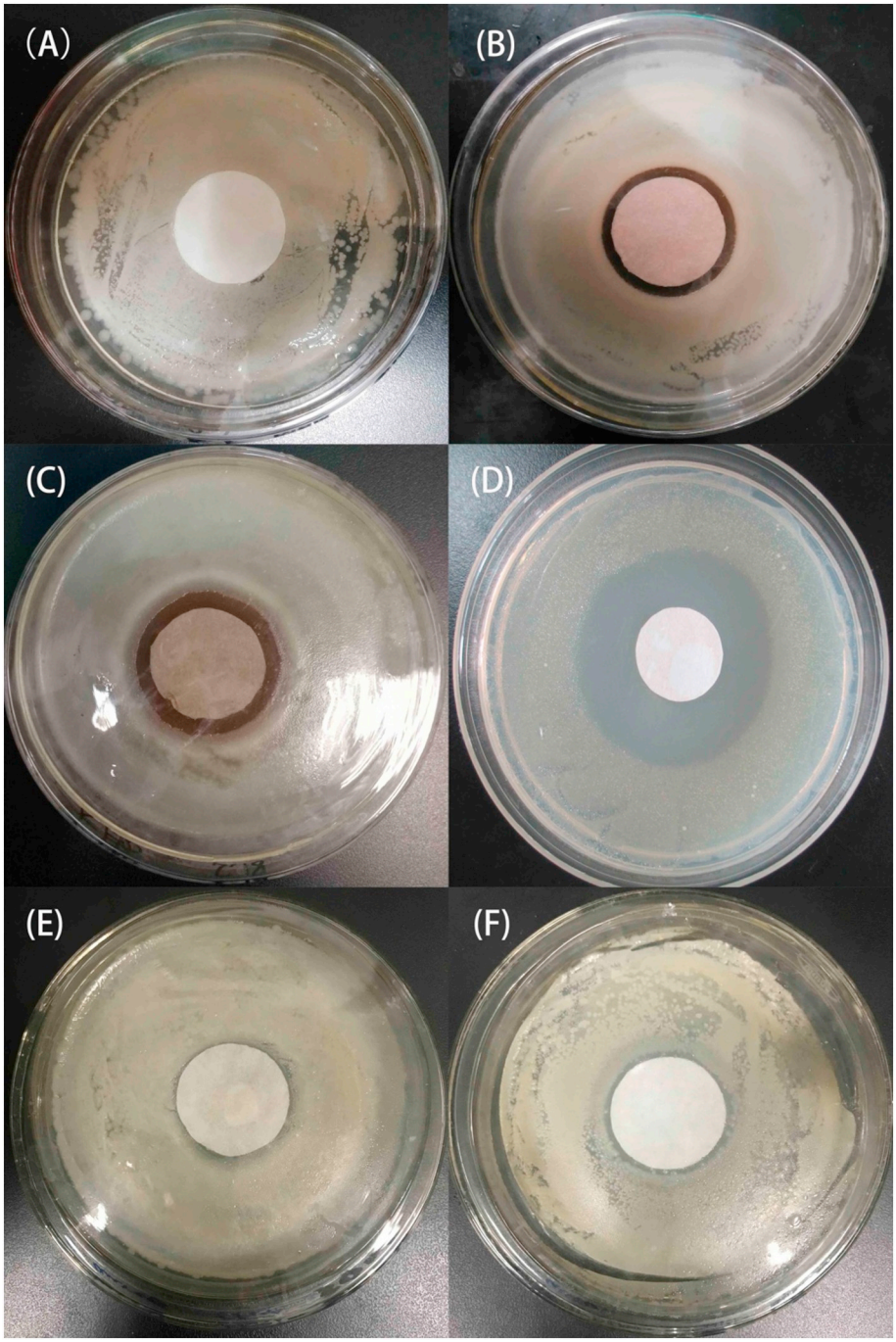

Fig. 6. The images of inhibition zones for different samples against *E. coli*. (A) 0 μg; (B) 5 μg [$Zn(CPDA)(NO_3)_2$)]; (C) 20 μg [$Zn(CPDA)(NO_3)_2$)]; (D) 20 μg gentamycin; (E) 20 μg CPDA; (F) 20 μg $Zn(NO_3)_2{\cdot}6H_2O$.

(1.0–2.0 $mg{\cdot}L^{-1}$) of **1**, which was not obviously different from that of negative control, but it was increased slowly at the concentration of > 20.0 $mg{\cdot}L^{-1}$. Thus, it could be attained that **1** had exerted its antibacterial effect in a concentration-dependent manner, suggesting that a higher concentration of **1** would result in superior inhibitory effect on the gram-negative and gram-positive bacteria. Simultaneously, the impact on incubation time is also presented in Fig. 5. It could be found that, after 24 h of culture in **1** solution, the OD value of the microorganism was slightly changed, illustrating that the growth of these two bacteria could be effectively inhibited by **1** during 24 h. Specifically, the minimum inhibitor concentration (MIC) of **1** for *E. coli* and *S. aureus* was calculated to be 8.0 mg/L based on the growth curves in this study.

In the disc diffusion assay of this study to determine the antibacterial activity of **1**, growth suppression could be observed in the plates (Fig.6 and Fig.7). Afterwards, no ZOI could be observed in negative control from Fig.6 (A), but a fairly large ZOI had appeared in positive group cultivated with gentamycin in Fig.6 (F). Specially, in Fig.6 (C), a relatively wide ZOI in plates could be observed after *E. coli* had been cultivated with **1** at high concentrations. By contrast, the formed ZOI was small in Fig.6 (B), revealing that low concentrations of **1** had less inhibitory effect on bacterial growth. These results demonstrated that the inhibition of **1** on bacterial growth was concentration-dependent; in other words, the ZOI was increased with the increase in **1** concentration. Analogously, the tendency for **1** against *S. aureus* was basically the same as that against *E.coli* (Fig.7 (A-F)), but the ZOI was a

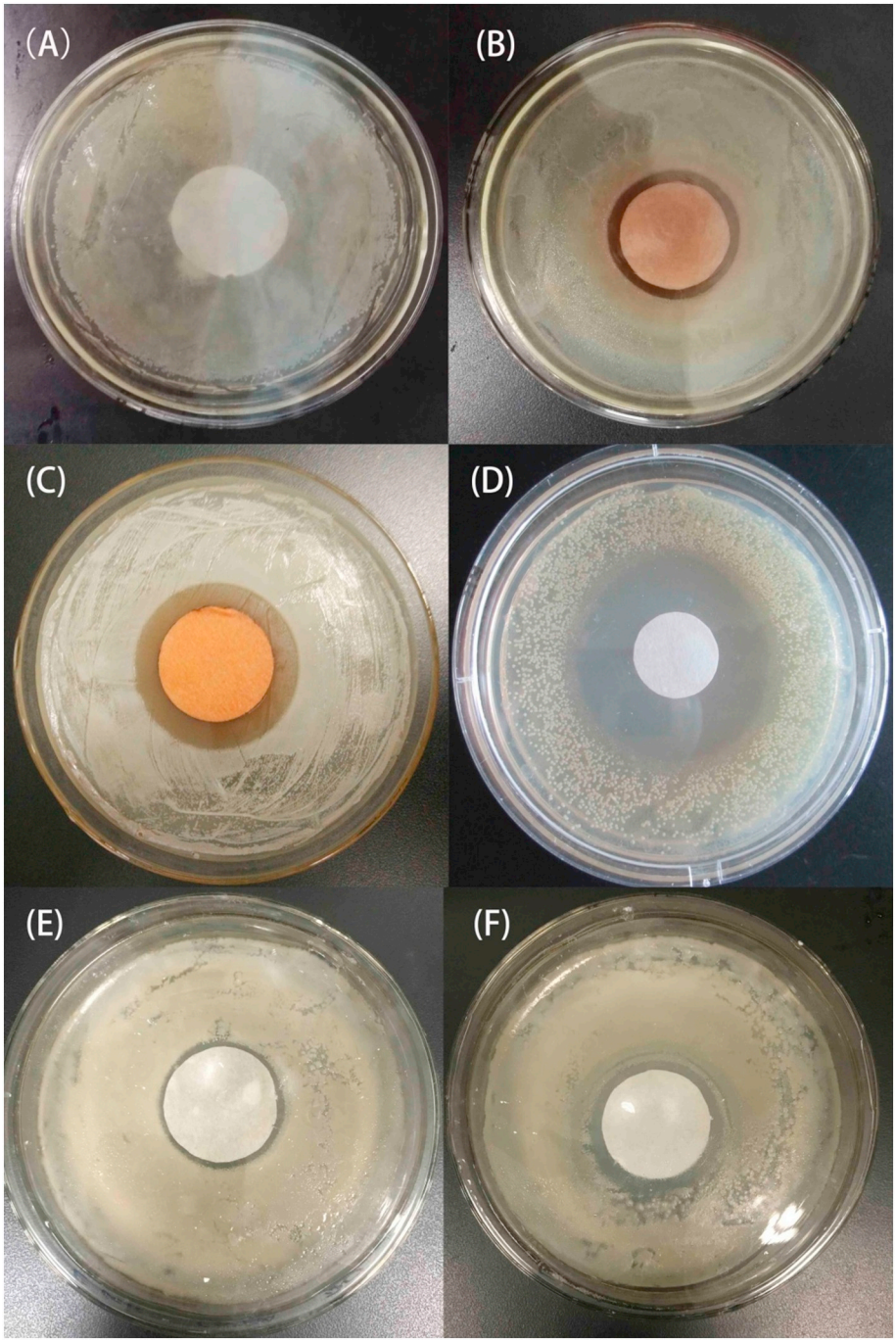

Fig. 7. The images of inhibition zones for different samples against *S. aureus*. (A) 0 μg; (B) 5 μg [Zn(CPDA)(NO_3)$_2$)]; (C) 20 μg [Zn(CPDA)(NO_3)$_2$)]; (D) 20 μg gentamycin; (E) 20 μg CPDA; (F) 20 μg Zn(NO_3)$_2$·6H_2O.

little larger than that of *E.coli* under the same condition. Obviously, these results were consistent with findings from the growth inhibition study, indicating that **1** had relatively effective antibacterial activity against *E. coli* and *S. aureus*. Moreover, both CPDA and zinc nitrate had also displayed antibacterial activities against *E.coli* and *S. aureus* (Fig.6 (D & E) and Fig.7 (D & E), suggesting that the high antibacterial activity of **1** might be resulted from the synergistic effects of CPDA and Zn^{2+}.

3.4. Mechanism of action

Though the precise mechanisms of metal CPs remain largely unclear at present, the generation of ROS may account for a possible mechanism for antibacterial activity, which has been reported by many researchers until now [29,31,32]. Therefore, to understand the mechanisms of antibacterial activity, ROS production was detected using the Reactive Oxygen Species Assay Kit. Hence, ROS production would be measured through qualitative assessment after incubating microorganisms with **1**. As exhibited in Fig.8, the fluorescent intensity was presented to analyze the intracellular ROS level of *E.coli* and *S. aureus*. It could be discovered from Fig.8 (a), the ROS levels generated by bacteria in negative control were very low. In comparison, it was apparent in Fig.8 (b-c) that bacteria treated with **1** had presented higher fluorescent intensity compared with that of negative control, which had indicated higher ROS levels formed in bacteria. The above-mentioned data mainly manifested that the toxic effects of **1** could be induced by the increased intracellular ROS levels.

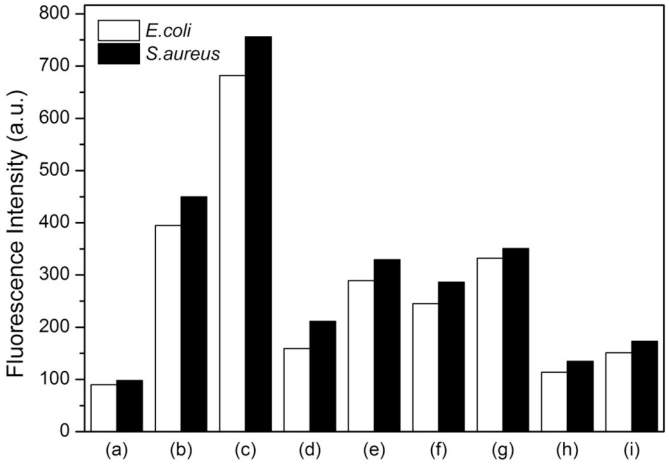

Fig. 8. The qualitative measurement to determine the effect of antioxidant on ROS generation in *E. coli* and *S. aureus* during 24 h. (a) 0 mg /L [Zn(CPDA)$(NO_3)_2$)]; (b) 8.0 mg /L [Zn(CPDA)$(NO_3)_2$)]; (c) 20.0 mg/L [Zn(CPDA)$(NO_3)_2$)]; (d) 20.0 mg/L CPDA; (e) 20.0 mg/L $Zn(NO_3)_2{\cdot}6H_2O$; (f) 1.0×10^{-2} mol/L NAC + 8.0 mg/L [Zn(CPDA)$(NO_3)_2$)]; (g) 1.0×10^{-2} mol/L NAC + 20.0 mg/L [Zn(CPDA)$(NO_3)_2$)]; (h) 1.0×10^{-2} mol/L NAC + 20.0 mg/L CPDA; (i) 1.0×10^{-2} mol/L NAC + 20.0 mg/L $Zn(NO_3)_2{\cdot}6H_2O$.

Furthermore, to confirm the antibacterial mechanism of **1** involved in ROS, its antibacterial activity had been evaluated under the action of *N*-acetylcysteine (NAC), as seen in Fig.8. Oxidative damage could be prevented by NAC [29,33], a valid antioxidant with a mercapto group. In NAC tests, when NAC was separately added to **1** at the concentrations of 8.0 and 20.0 mg/L, respectively, the fluorescent intensities were markedly reduced. These series of experiment results proved that the antibacterial activity of **1** was weakened under the action of antioxidants, further demonstrating that ROS was largely related to the antibacterial activity, which had actually played a vital role in the antibacterial mechanism of **1**. Moreover, when NAC was separately added to the CPDA or Zn^{2+} solution, the fluorescent intensities were also reduced, confirming that the generation of ROS was involved by CPDA and Zn^{2+} in the antibacterial activity.

4. Conclusions

To sum up, the Zn(II)-based CP [Zn(CPDA)$(NO_3)_2$)] (**1**) had been successfully synthesized through the solvothermal reaction, with 1,2-cyclopentanedicarboxylic acid (CPDA) being used as the ligand. Through a series of antibacterial experiments, our results revealed that **1** had displayed comparatively high antibacterial activities against gram-negative (*E.coli*) and positive bacteria (*S. aureus*) in a concentration-dependent manner. Additionally, the potential antibacterial mechanism could be attributed to the formation of its intracellular ROS. Therefore, **1** might show promising application prospects as an antibacterial agent, which might facilitate the application in medical and biological fields against resistant bacteria to some extent.

Acknowledgement

This work was supported by National Natural Science Foundation of Guangdong Province (No.2017A030310666 and No.2018A030307003), Nanhai Marine Biomedical Resources of Public Service Platform Fundation of Guangdong Medical University (No.2HC18013 and No.2HC18016), Science & Technology Foundation of Dongguan City (No.2015108101014), Medical Science and Technology Development Foundation of Guangdong Province (No.A2016355), Undergraduate Science & Technology Innovation Cultivate Special Funds of Guangdong Province (No.pdjhb0228).

References

[1] K. Becker, Y. Hu, N. Biller-Andorno, Int. J. Med. Microbiol. 296 (2006) 179–185.
[2] J. Lee, O.K. Farha, J. Roberts, K.A. Scheidt, S.T. Nguyen, J.T. Hupp, Chem. Soc. Rev. 38 (2009) 1450–1459.
[3] C.C. Wang, J.R. Li, X.L. Lv, Y.Q. Zhang, G. Guo, Energy Environ. Sci. 7 (2014) 2831–2867.
[4] K.M. Taylor-Pashow, J.D. Rocca, Z. Xie, S. Tran, W. Lin, J. Am. Chem. Soc. 131 (2009) 14261–14263.
[5] L. Sorace, C. Benelli, D. Gatteschi, Chem. Soc. Rev. 40 (2011) 3092–3104.
[6] W.J. Li, J. Lu, S.Y. Gao, Q.H. Li, R. Cao, J. Mater. Chem. A 2 (2014) 19473–19478.
[7] B. Gole, A.K. Bar, P.S. Mukherjee, Chem. Commun. 47 (2011) 12137–12139.
[8] E.M. Dias, C. Petit, J. Mater. Chem. A 3 (2015) 22484–22506.
[9] G. Wyszogrodzka, B. Marszałek, B. Gil, P. Dorożyński, Drug Discov. Today 21 (2016) 1009–1018.
[10] Y. He, J. Shang, Q. Gu, G. Li, J. Li, R. Singh, P. Xiao, P.A. Webley, Chem. Commun. 51 (2015) 14716–14719.
[11] S. Kitagawa, R. Matsuda, Coord. Chem. Rev. 251 (2007) 2490–2509.
[12] S. Sorribas, B. Zornoza, C. Téllez, J. Coronas, Chem. Commun. 48 (2012) 9388–9390.
[13] K.C. Gupta, H.K. Abdulkadir, J. Macromol. Sci. A 45 (2008) 53–64.
[14] N. Chantarasiri, N. Sutivisedsak, C. Pouyuan, Eur. Polym. J. 37 (2001) 2031–2038.
[15] I.F. Abu-Awwad, F.I. Khalili, B.A. Sweileh, Solvent Extr. Ion Exch. 28 (2010) 682–705.
[16] T. Ahamad, S.M. Alshehri, Bioinorg. Chem. Appl. (2010) 1–7.
[17] X. Lu, J. Ye, Y. Sun, R.F. Bogale, L. Zhao, P. Tian, G. Ning. Dalton Trans.. 43 (2014) 10104–10113.
[18] V. Violet Dhayabaran, T. Daniel Prakash, R. Renganathan, Elsa Friehs, Detlef W. Bahnemann. J. Fluoresc. 27(2016)135–150.
[19] H. Hu, W. Zhang, Y. Qiao, X. Jiang, X. Liu, C. Ding. Acta Biomater. 8(2012) 904–915.
[20] K. Huo, X. Zhang, H. Wang, L. Zhao, X. Liu, P.K. Chu, Biomaterials 34 (2013) 3467–3478.
[21] L. Taghizade, M. Montazerozohori, A. Masoudiasl, S. Joohari, J.M. White, Mater. Sci. Eng. C Mater. Biol. Appl. 77 (2017) (229–224).
[22] H. Ma, E.T. Darmawan, M. Zhang, L. Zhang, J.D. Bryers, J. Control. Release 172 (2013) 1035–1044.
[23] M.K. Stathopoulou, C.N. Banti, N. Kourkoumelis, A.G. Hatzidimitriou, A.G. Kalampounias, S.K. Hadjikakou, J. Inorg. Biochem. 181 (2018) 41–55.
[24] M. Aldabaldetrecu, L. Tamayo, R. Alarcon, M. Walter, E. Salas-Huenuleo, M.J. Kogan, J. Guerrero, M. Paez, M.I. Azócar, Molecules 23 (2018) 1629.
[25] J.F. Zhang, J.J. Wu, G.D. Tang, J.Y. Feng, F. Luo, B. Xu, C. Zhang, Sensors Actuators B Chem. 272 (2018) 166–174.
[26] S. Jadhav, S. Gaikwad, M. Nimse, A. Rajbhoj, J. Clust. Sci. 22 (2011) 121–129.
[27] A.J. Kora, J. Arunachalam, World J. Microbiol. Biotechnol. 27 (2011) 1209–1216.
[28] S.K. Mahto, C. Park, T.H. Yoon, S.W. Rhee, Toxicol. in Vitro 24 (2010) 1070–1077.
[29] H.Y. Xu, F. Qu, H. Xu, W.H. Lai, Y.A. Wang, Z.P. Aguilar, H. Wei, Biometals 25 (2012) 45–53.
[30] X. Wang, S. Liu, M. Li, P. Yu, X. Chu, L. Li, G. Tan, Y. Wang, X. Chen, Y. Zhang, C. Ning, J. Inorg. Biochem. 163 (2016) 214–220.
[31] M.P. Brynildsen, J.A. Winkler, C.S. Spina, I.C. Macdonald, J.J. Collins, Nat. Biotechnol. 31 (2013) 160–165.
[32] T. Zoltan, F. Vargas, V. López, V. Chávez, C. Rivas, Á.H. Ramirez, Mol. Biomol. Spectrosc. 135 (2015) 747–756.
[33] G. Salazar, J. Huang, R.G. Feresin, Y. Zhao, K.K. Griendling, Free Radic. Biol. Med. 108 (2017) 225–235.